

Phase selective growth of Ge nanocrystalline films by ionized cluster beam deposition technique and photo-oxidation study

S. Mukherjee¹, A. Pradhan¹, T. Maitra², S. Mukherjee², A. Nayak², S. Bhunia^{1*}

¹Surface Physics and Material Science Division, Saha Institute of Nuclear Physics, HBNI, 1/AF, Bidhannagar, Kolkata-700064, India

²Department of Physics, Presidency University, 86/1, College Street, Kolkata-700073, India

*Corresponding author: Tel: (+91) 33 2337 5348; E-mail: satyaban.bhunia@saha.ac.in

Received: 21 October 2016, Revised: 29 December 2016 and Accepted: 23 January 2017

DOI: 10.5185/amlett.2017.1462

www.vbripress.com/aml

Abstract

In this paper, we report the possibility of phase-selective growth of Ge nanocrystals by changing the kinetic energy of the clusters in an ionised cluster beam deposition system. Typically, the films are of mixed phase of normal cubic and high energy tetragonal structures, the relative proportion of which could be controlled by controlling the ionisation and applied accelerating potential as has been confirmed from Raman spectroscopic study. The films deposited using neutral clusters showed higher yield of the tetragonal phase with nanocrystallites of diameter ~ 7 nm as evidenced from HRTEM data. The optical bandgap of the nanocrystals were observed to be blue shifted upto 1.75 eV compared to the bulk Ge attributing to the presence of Ge tetragonal ST-12 phase and the resulted quantum confinement effect inside the nanocrystals. The tetragonal-rich films were further studied by controlled photo-oxidation to tune their optical band gap. A visible photoluminescence due to excitonic transitions have been observed from the as-grown Ge film enriched in tetragonal phase with average crystallite size ~ 7 nm. The photoluminescence peak was further blue shifted after the course of photo-oxidation due to reduced nanocrystallite size. Copyright © 2017 VBRI Press.

Keywords: Ge Nanocrystals, ionized cluster beam, tetragonal, diamond-like, photo-oxidation, photoluminescence.

Introduction

Ge nanocrystals (Ge-NC) are one of the interesting semiconductor materials extensively studied for its unique visible light emission and electrical properties which are distinct from that of the bulk semiconductors [1-5]. Relaxation of momentum selection rules of the three-dimensionally confined carriers inside the nanostructures gives rise to intense radiative transitions [6]. Bulk Ge in normal diamond structure is not very useful for optoelectronic device applications because of its small indirect band gap. However, it can also exist in tetragonal form (ST-12) under high pressure, as reported by Saito (1979) in Ge particles of size < 20 nm [3]. Kanemitsu et. al. reported growth of Ge-NC of size less than 4 nm which deviated from the usual diamond-like structure, showing the characteristics of a direct transition and exhibited visible photoluminescence [7]. Sato et. al. reported a blue shift of absorption band edge of tetragonal-Ge up to 2 eV in 4.3 nm size particles [7, 8]. Theoretically, nanoparticles with normal diamond-like structure can exhibit the phase transition to tetragonal structure to reduce its surface energy when the particle size goes below a certain threshold value [9]. Tetragonal

Ge is more suitable for optoelectronic applications due to its predicted direct band gap of 1.47 eV at room temperature [10]. Recently, the tetragonal phase of Ge has been found to be a promising candidate to substitute current carbonaceous anodes of lithium ion batteries owing to its stronger binding interactions with Li atoms [11].

There have been a few techniques such as gas aggregation in He or Ar [12], cluster beam deposition [7], laser ablation [13], ion implantation [14], magnetron sputtering [2], chemical vapor deposition [15], solution phase synthesis [16, 17] etc. to grow Ge-NCs, which can control the size of the crystallites [8]. But most of these techniques yield Ge-NCs in conventional cubic phase. By employing ionized cluster beam deposition (ICB) technique, it is possible to selectively grow Ge-NCs as a mixture of both tetragonal and cubic phases [18] by physically adjusting the kinetic energy of the deposited clusters [19]. Thus, the present work is an attempt to achieve high yield of tetragonal Ge-NCs by employing ICB deposition method. This technique was first reported by Takagi et al to grow atomically smooth metallic thin films on various substrates and was later extended for other applications [8, 17, 20]. In this technique, a beam of

adiabatically cooled clusters of Ge atoms in vapor phase is ionized and subjected to different accelerating potentials and finally nucleates into NCs of different size on the substrate depending on their respective kinetic energy [20]. For NC size below a critical value, a strain-induced phase transformation takes place in the grown Ge surface layers which transforms its cubic form into a high energy metastable tetragonal phase [9, 17, 20, 21].

Moreover, to achieve emission of visible light from the Ge-NCs it is necessary to tune their bandgap. Previously, visible photoluminescence has been reported from Ge nanocrystalline structure of size less than 4 nm in tetragonal phase showing the characteristics of a direct transition [7]. A blue photoluminescence was observed from Ge-NCs embedded in SiO₂ matrix [8, 19, 22]. The Ge-NCs can undergo a controlled photo-oxidation by suitable exposure to light [7]. When the grown Ge-NC films are photo-oxidized, layers of GeO_x are formed very slowly at the expense of Ge surface atoms which reduce the average crystallite size [23-25]. There have been reports of size reduction by this method on other NCs, such as CdSe/ZnS quantum dots [23]. Other oxidation methods are uncontrollably fast processes which can oxidize the entire NCs. With decrease in crystallite size, quantum confinement effect becomes more prominent resulting in enhanced optical bandgap of the Ge NCs [25, 26]. With the abundance of comparatively higher energy tetragonal phase of Ge (Tetragonal ST-12), it is rather easier to photo-oxidize the NCs with UV excitation and tune its emission wavelength to the visible region by controlling the time of exposure [26]. The Ge-NCs under the oxide layers with suitable degree of photo-oxidation have the potential to be good emitter of visible light [25].

In this paper, we report a novel phase-selective growth of Ge-NC films by employing ICB deposition technique. Our results show the possibility to selectively grow tetragonal Ge phase of crystallite size ~7 nm by varying the ion energy of the clusters in the ICB deposition chamber. By varying the relative proportion of the two phases, it is also possible to tune the spectral properties of Ge-NCs. The tetragonal phase not only exhibited visible photoluminescence emission but its optical emission could also be tuned to varying degree of quantum confinement by controlled photo-oxidation.

Experimental

A set of Ge-NC films with different relative phase composition were grown using both neutral and ionized Ge beam in the ICB deposition system on quartz substrates kept at liquid nitrogen temperature. Ge powder loaded inside confined cylindrical graphite crucible (thickness 1 mm, length 14 mm and diameter 8 mm) has been heated to high temperature through a resistive coil surrounding the outer surface of the crucible. The produced Ge vapor (99.998% pure) is made to eject supersonically through a small nozzle (diameter 0.5 mm) into a vacuum chamber (4x10⁻⁶ Torr) which undergoes adiabatic expansion and subsequently cooled to form super atoms or clusters (containing 100-2000 atoms). The

beams of neutral and ionized clusters are directed to the substrate surface maintained at a low temperature. The beam of neutral atoms impinges on the substrate and neutral Ge nanocrystalline films (Film-1) are grown. For ionized Ge-NC films (Film-2 and Film-3), the clusters were ionized by electron impact and subsequently accelerated to the quartz substrate by subjecting to externally maintained accelerating potentials (V_a) of 1.5 kV and 2.5 kV, respectively. The relative phase proportion of Ge inside the grown NCs can be varied by controlling the ionization and accelerating potential in ICB system. The crucible and substrate were kept apart by a distance of 120 mm. The growth rate was monitored by a crystal oscillator and was kept constant at ~0.03 nm/s. The microstructural study of the grown nanocrystalline films were carried out using high resolution electron transmission microscopy (JEM2100, JEOL) at an operating voltage of 300 KV under cross-sectional geometry. The films were then photo-oxidized in H₂O₂ atmosphere at room temperature using UV light ($\lambda = 242$ nm) for 30-60 minutes and studied using PL and optical absorption measurements. Further, the photo-oxidized Ge films were etched (removing the grown oxide layers) by using aqueous HF (HF: H₂O = 40:60) solution. PL and X-ray photoelectron spectroscopy (XPS) measurements were carried out on these films to understand the role of oxide layers to the light emission process.

Results and discussion

The comparative Raman spectra of the three Ge-NC films grown using neutral cluster (Film-1), and with applied potentials of 1.5kV (Film-2) and 2.5kV (Film-3) is shown in **Fig. 1**. A TO-like broadened red shifted phonon peak appeared at ~275 cm⁻¹ in addition to the phonon peak at ~300 cm⁻¹ in the spectra of all the three films. The Raman peak at ~300 cm⁻¹ is very close to that of bulk Ge and is associated with diamond-like cubical Ge phase (Γ_{25}) [22,27]. The broadened red shifted phonon peak is attributed to the confinement of phonons inside very small crystallites due to its encounter with a grain boundary. This is the signature of emergence of a different phase of Ge having smaller grain size, co-existing with cubic Ge phase. With the reduction of accelerating potential (V_a) i.e., low kinetic energy of the clusters, applied on the Ge cluster beam, the intensity of the red shifted peak (~275 cm⁻¹) enhances owing to the gradual increment of relative proportion of this new phase. The red shifted peak becomes the most prominent for the films grown by depositing neutral clusters (Film-1) where the relative content of that new phase of Ge is maximum. The peak intensity corresponding to the cubic Ge phase is the least for Film-1 and gets gradually enhanced with increasing accelerating potential. This second phase of Ge has appeared significantly inside nanocrystallites of size ~7 nm. The average size of the nanocrystallites are ~7 nm, ~10 nm and ~15 nm for the Film-1, Film-2 and Film-3 respectively as estimated from the position of their respective Raman peaks related to localized optical phonons [6, 28].

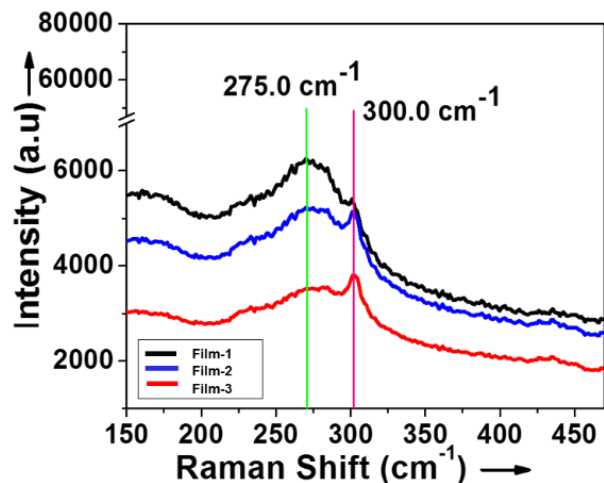


Fig. 1. Comparative Raman Spectra of the films deposited using neutral Ge clusters (Film-1) and using ionized Ge clusters (Film-2, Film-3) under accelerating potentials of 1.5 and 2.5 KV.

Variation of crystalline properties of the films was studied from the high-resolution transmission electron microscopic (HRTEM) images and selected area electron diffraction (SAED) pattern of the Film-1 and Film-2 as shown in **Fig. 2(a)-(d)**. The TEM images clearly depict the appearance of lattice fringes marked by encircled regions for both the films as shown in **Fig. 2(a)** and **Fig. 2(c)**, whereas the corresponding high resolution lattice images are shown in **Fig. 2(b)** and **Fig. 2(d)**. Short range orientations of nanocrystallites in different directions is clearly visible in Film-2 which is almost absent in Film-1. The mean value of the crystallite size distributions of the two films are ~ 7 nm and ~ 11 nm, respectively, which agree well with the microstructural measurements using Raman spectroscopy [29]. The lattice spacings were also (d_{hkl}) calculated from the radii of the rings in the SAED pattern shown in **Fig. 2(b)** and **Fig. 2(d)**, corresponding to Film-1 and Film-2, respectively. For the Film-1, the calculated d-values 0.3514 nm and 0.265 nm correspond to the (111) and (210) lattice planes of Ge in closely packed tetragonal structure (ST-12) respectively [30-32]. For the Film-2, the observed rings (**Fig. 2(d)**) correspond to the (111), (311) and (331) lattice planes of normal cubic diamond-like structure having d-values of 0.3267 nm, 0.2 nm, 0.1705 nm and 0.1298 nm respectively [3]. The Film-2 shows higher crystallinity than neutral Ge-NC Film-1 as was evident from the brighter spots on the rings in SAED pattern of Film-2 which is more ordered owing to the relative abundance of cubic Ge phase.

The optical absorption spectra of the three types of Ge-NC films viz. Film-1, Film-2 and Film-3 are shown in **Fig. 3**. We observed a substantial blue shift of the absorption edge of the cluster beam deposited films relative to the bulk band gap of Ge. The values of optical bandgap, calculated from the conventional $(\alpha h\nu)^2$ vs $h\nu$ plot, shown in the inset of **Fig. 3** are 1.75 eV, 1.60 eV and 1.55 eV for the Film-1, Film-2 and Film-3, respectively. The largest band gap is observed for the film grown using neutral clusters due to the presence of large fraction of tetragonal phase, which

has larger band gap compared to the cubic phase. The shifting of the absorption threshold towards lower energy with increasing ion energy during the film deposition with ionized Ge cluster beam is due to the incorporation of larger fraction of cubic Ge phase. Quantum confinement of carriers inside the nanocrystals plays a dominant role for widening the band gap as is evident from the observed gradual blue shift of absorption band edges with the decreasing nanocrystallite size [33].

Usually, bulk Ge crystallizes in cubic diamond-like structure. But, while depositing the films by beam of Ge clusters, a mechanical strain is induced in the grown Ge layers by compressive stress due to large lattice misfit between Ge and substrate material [34].

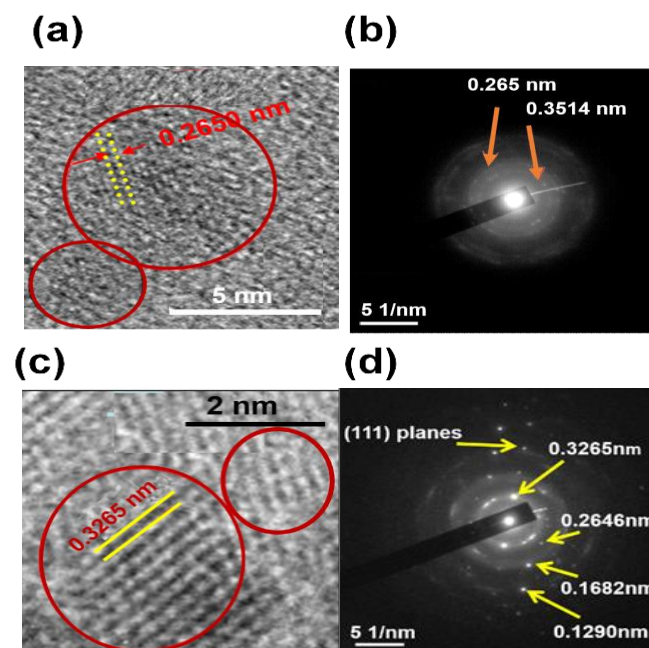


Fig. 2 (a) Cross-sectional High resolution lattice image and (b) the SAED pattern for the Ge-NCs Film-1, whereas (c) and (d) show corresponding similar images for Film-2. Short range orientations in different directions are much more prominent in Film-2 than Film-1 as represented by encircled regions.

For NC size below a certain critical value, the increased strain energy can be released by transforming unstable cubic Ge phase into metastable tetragonal ST-12 structure and eventually it got crystallized in tetragonal structure [35]. When the clusters are ionized, the stored electrostatic energy can significantly reduce the effect of surface and help the crystallites to grow in the cubic form. Application of accelerating potential to the charged clusters causes them to impinge on the substrate with higher kinetic energy and coagulate with other clusters into relatively bigger NCs, as has been observed in the TEM images of Film-2. The photo-oxidation study reported here was mainly on the films grown using neutral cluster (Film-1) only, because these contain larger proportion of tetragonal phase which incorporate a high density of unsaturated bonds [10, 33] and having loosely bound atoms. This facilitates photo-oxidation efficiently

compared to the other films (Film-2 and Film-3) under the same UV exposure.

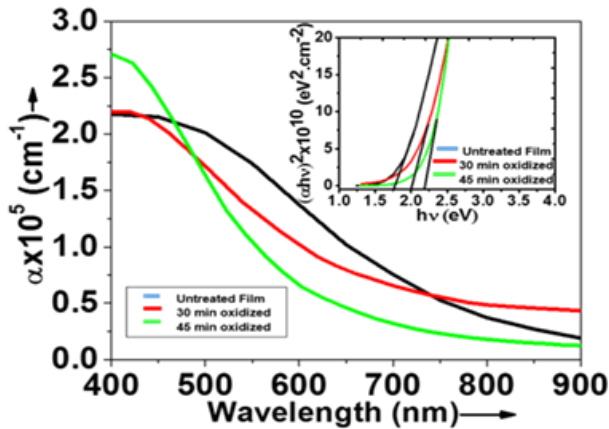


Fig. 3 Optical absorption spectra of Ge nanocrystalline films.

Inset: Plot of $(\alpha hv)^2$ vs hv . The intersections of the dotted lines with the energy axis gives approximate values of optical gaps as 1.75 eV, 1.60 eV and 1.55 eV for Film-1, Film-2 and Film-3 respectively.

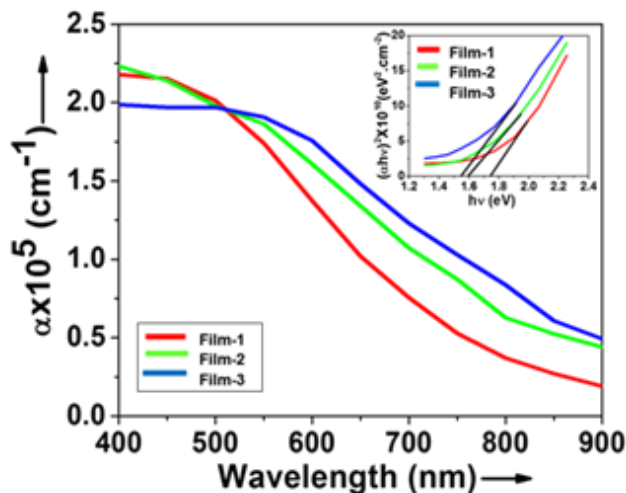


Fig. 4 Optical absorption spectra of the Film-1 in three different conditions: as-grown, 30 minute photo-oxidized and 45 minute photo-oxidized. *Inset:* Plot of $(\alpha hv)^2$ vs hv . Estimated absorption band edge are ~ 1.75 eV, ~ 2 eV and ~ 2.25 eV.

Three-dimensional carrier confinement inside very small sized NCs plays a significant role for reducing the effective conduction band offset between Ge cores and surrounding GeO_x layers for the photo generated carriers (mostly generated inside Ge) according to the model of photon induced oxidation enhancement proposed by Young [8]. In our sample, the Photo-oxidation was carried out for two different UV exposure times, viz., 30 minutes and 45 minutes. The absorption edge was found to increase from 1.75 eV (as grown unexposed film) to ~ 2 eV and ~ 2.25 eV, respectively for the samples subjected to two UV exposure times, as shown in optical absorption spectra (Fig. 4). This blueshift of optical bandgap indicates gradual shrinking of Ge-NC core size [23]. On the other hand, the simultaneous formation of GeO_x due to photo-oxidation may also cause a successive widening of the energy gap involving the conversion of more

number of Ge-Ge bonds to Ge-O-Ge configuration in the photo-oxidation process. The continuous blue shift with the increasing degree of photo-oxidation would be a homogeneous process and its contribution to increased bandgap cannot be ruled out at this stage [22, 24].

To understand surface oxidation state of the photo-oxidized Ge-NC films, we carried out XPS measurements on Film-1 by using $\text{AlK}\alpha$ x-ray source ($E=1486.6$ eV). Fig. 5 shows three XPS spectra of Ge-3d peak of the as-grown films, the photo-oxidized films and the films immediately after removing the grown oxide by aqueous HF treatment as indicated by red, green and black colored curves respectively. In each spectrum, two pronounced peaks are found at 29.3 eV from Ge-3d core electrons and at ~ 32 eV corresponding to germanium oxide. Deconvoluting the spectra of as-grown air-exposed film (inset of Fig. 5) shows the oxide related peak at 31.8 eV with a chemical shift of 2.5 eV due to Ge^{+3} oxidation state. Similar analysis for the photo-oxidized sample showed the corresponding peak at 32.6 eV (3.3 eV chemical shift) which is due to the Ge^{+4} oxidation state [36]. The XPS spectra of the HF treated surface showed a strong Ge-3d core level peak and a very weak oxide related peak, indicating removal of the grown oxide due to this treatment.

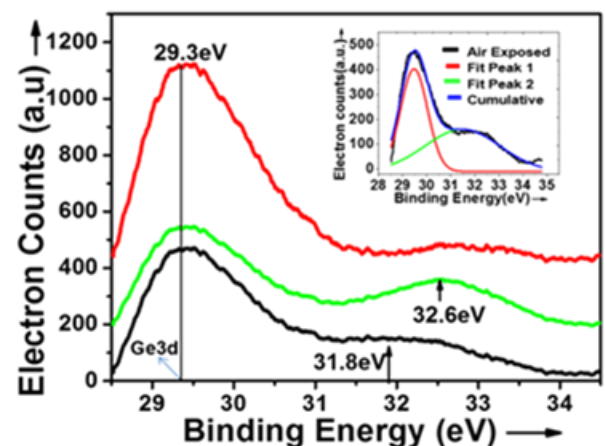


Fig. 5. XPS spectra of Film-1 under three different environment: air exposed (Black), UV photo-oxidized (Green) and treated with aqueous HF solution for 30s (Red). *Inset:* Gaussian deconvoluted XPS peaks of air-exposed Film-1.

The comparative room temperature (RT) PL spectra from the as-grown Film-1 and 30-minute photo-oxidized Film-1 excited by 514 nm Ar+ laser is shown in Fig. 6. Both the PL spectrum show multi-peak structures which are properly fitted using Gaussian line shapes. Bandgap related transitions were detected at ~ 1.74 eV and ~ 2.06 eV from the as-grown and photo-oxidized films respectively at RT which are in good agreement with the values of their absorption band edges estimated from optical absorption spectra.

These transitions are rather suppressed by other intense luminescence [7] in the visible range 1.56-1.67 eV and 1.82-1.95 eV for the as-grown and photo-oxidized films respectively. These optical transitions are more likely to

be ascribed to bound excitons in Ge NCs [37, 38] rather than originating from free electron-hole pair recombination due to profound quantum confinement effect inside the Ge NCs that would shift the bandgap to higher values [39]. This is indeed a signature of nanostructured quantum dots [40]. For the photo-oxidized film, all the peaks have been blue shifted almost by the same amount of 300 meV from that of as-grown film owing to the reduction of NC core size under GeO_x layers [7, 24]. The effect of excitons increases with increasing quantum size effect as is evident from more dominant excitonic PL peaks for photo-oxidized film compared to that of as-grown film [25-26]. The bandwidth of the PL peaks of the photo-oxidized films have been observed to increase than that before photo-oxidation, which clearly suggests more dispersed NC-core size distribution due to oxidation. Sub-oxide layers of Ge may also play a role of luminescent centers which emits blue light at ~3.1 eV [41-43]. But that emission is far beyond the range of our PL spectra. So the contribution of GeO_x layers to luminescence can be ruled out.

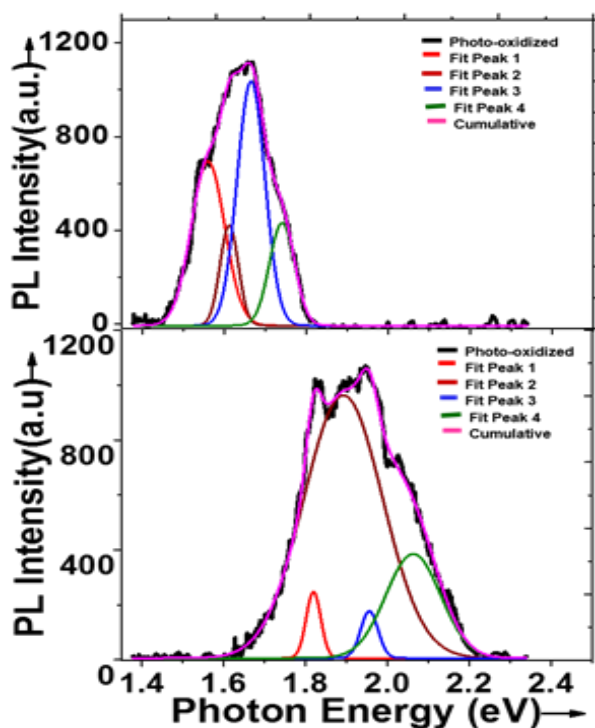


Fig. 6. PL spectra of Film-1: as-grown (top) and 30mins photo-oxidized (bottom). The black lines correspond to the experimental data of the two films. The multiple peaks are fitted by Gaussian line shapes represented by the colored lines.

Conclusion

In this paper we have reported a phase-selective growth of Ge NCs films by employing an ionized cluster beam deposition technique. Typically, all the films were composed of cubic diamond-like and tetragonal phases. We have categorically shown a controlled yield of a particular phase by controlling the kinetic energy of the impinging clusters on the substrates. Films grown using

neutral clusters (low kinetic energy) showed tetragonal structure as the dominant phase with nanocrystallite size of the order of 7 nm. The ratio of tetragonal to cubic structure decreased with increasing kinetic energy of the cluster beam. By varying the relative proportion of the two phases, it is also possible to tune the spectral properties of Ge NCs. In addition to strong optical absorption, the film showed room temperature photoluminescence in the visible region. We have also studied the possibility of controlled UV photo-oxidation of the tetragonal-rich films to further reduce the crystallite size and thereby further tuning of the optical emission energy. Apart from optoelectronics, the Ge-NC in the tetragonal phase also finds application as an alternative anode in Li ion batteries.

Acknowledgements

Special thanks to Unit on Nano.Sc. IACS, Kolkata, India.

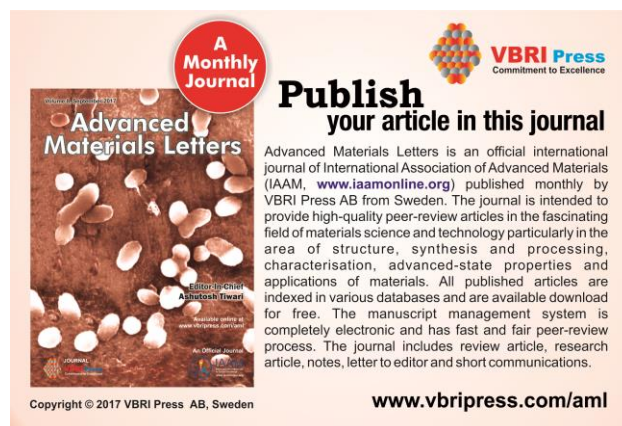
Author's contributions:

Conceived the plan: SB, AN. Authors SM, AP, TM and SM contributed equally in the work. Authors have no competing financial interests.

References

1. Takeoka, S.; Fujii, M.; Hayashi, S.; and Yamamoto, K.; *Phys. Rev. B*, **1998**, *58*, 7921.
DOI: [10.1063/1.829\(98\)09535-6](https://doi.org/10.1063/1.829(98)09535-6)
2. Maeda, Y.; Tsuamoto, Y.; Yazawa, Y.; Kanemitsu, Y. and Masumoto, Y.; *Appl. Phys. Lett.*, **1991**, *59*, 3168.
DOI: [10.1063/1.105773](https://doi.org/10.1063/1.105773)
3. Saito, Y.; *J. Cryst. Growth*, **1979**, *47*, 61.
DOI: [10.1016/0022-0248\(79\)90157-X](https://doi.org/10.1016/0022-0248(79)90157-X)
4. Joannopoulos, J. D.; and Cohen, M. L., *Phys. Rev. B*, **1973**, *7*, 2644.
DOI: [10.1103/PhysRevB.7.2644](https://doi.org/10.1103/PhysRevB.7.2644)
5. Zacharias, M.; and Faucet, P. M., *Appl. Phys. Lett.*, **1997**, *71*, 380.
DOI: [10.1063/1.119543](https://doi.org/10.1063/1.119543)
6. Batra, Y.; Kabiraj, D., and Kanjilal, D., *Solid State Commun.*, **2007**, *143*, 213.
DOI: [10.1016/j.ssc.2007.07.014](https://doi.org/10.1016/j.ssc.2007.07.014)
7. Kanemitsu, Y.; Uto, H.; and Masumoto, Y.; Maeda, Y.; *Appl. Phys. Lett.*, **1992**, *61*, 2187.
DOI: [10.1063/1.113714](https://doi.org/10.1063/1.113714)
8. Sato, S.; Nozaki, S.; Morisaki, H. and Iwase, M., *Appl. Phys. Lett.*, **1995**, *66*, 3176.
DOI: [10.1063/1.113714](https://doi.org/10.1063/1.113714)
9. Tomanek, D.; and Schluter, M. A., *Phys. Rev. B.*, **1987**, *36*, 1208.
DOI: [10.1103/PhysRevB.36.1208](https://doi.org/10.1103/PhysRevB.36.1208)
10. Joannopoulos, J. D. and Cohen, M. L., *Solid State Commun.*, **1972**, *11*, 549.
DOI: [10.1016/0038-1098\(72\)90123-8](https://doi.org/10.1016/0038-1098(72)90123-8)
11. Cho, Y.J; Im, H.S; Kim, H.S.; Myung, Y; Back, S.H.; Lim, Y.R.; Jung, C.S.; Jang, D.M.; Park, J.; Cha, E.H.; Cho, W.I.; Shojaei, F. and Kang, H.S., *ACS Nano*, **2013**, *7*, 9075.
DOI: [10.1021/nn403674z](https://doi.org/10.1021/nn403674z)
12. Bostedt, C. et al.; *J. Phys.: Condens. Matter*, **2003**, *15*, 1017.
DOI: [10.1063/1.152630](https://doi.org/10.1063/1.152630)
13. Zhu, J.G., et al.; *J. Appl. Phys.*, **1995**, *78*, 4386.
DOI: [10.1063/1.359843](https://doi.org/10.1063/1.359843)
14. Ngiam, S.T., et al.; *J. Appl. Phys.*, **1994**, *76*, 8201.
DOI: [10.1063/1.357878](https://doi.org/10.1063/1.357878)
15. Nogami, M. and Abe Y.; *Appl. Phys. Lett.*, **1994**, *65*, 2545.
DOI: [10.1063/1.112630](https://doi.org/10.1063/1.112630)
16. Wilcoxon, J.P., et al.; *Phys. Rev. B*, **2001**, *64*, 035417.
DOI: [10.1103/PhysRevB.64.035417](https://doi.org/10.1103/PhysRevB.64.035417)
17. Yamada, I.; Takaoka, G. H., *Jpn. J. Appl. Phys.*, **1993**, *32*, 2121.

- DOI: [1347-4065/32/5R/2121](https://doi.org/10.1007/1347-4065/32/5R/2121)
18. Nozaki, S.; Sato, S. Rath, S.; Ono, H.; Morisaki, H.; *Bull. Mater. Sci.*, **1997**, *22*, 377.
DOI: [10.1007/BF02749945](https://doi.org/10.1007/BF02749945).
19. Gorokhov, E.B.; Volodin, V.A.; Marin, D.V. et al., *Semiconductors*, **2005**, *39*, 1168.
DOI: [10.1134/1.2085265](https://doi.org/10.1134/1.2085265)
20. Takagi, T., *Z. Phys. D. Atoms, Molecules and Clusters*, **1986**, *3*, 271.
DOI: [10.1007/BF01384816](https://doi.org/10.1007/BF01384816)
21. Kim, S. J. et al, *J. Mater. Chem*, **2010**, *20*, 331.
DOI: [10.1039/B915841C](https://doi.org/10.1039/B915841C)
22. Sato, S.; Nozaki, S.; and Morisaki, H., *J. Appl. Phys.*, **1997**, *81*, 1518.
DOI: [10.1063/1.363917](https://doi.org/10.1063/1.363917)
23. Sark, W. V. et al., *J. Phys. Chem. B*, **2001**, *105*, 8281
DOI: [10.1021/jp012018h](https://doi.org/10.1021/jp012018h)
24. Armatas, G. S. and. Kanatzidis, M. G, *Nature (London, U. K.)*, **2006**, *441*, 1122.
DOI: [10.1038/nature04833](https://doi.org/10.1038/nature04833)
25. Shi, X. et al., *J. Nanopart. Res.*, **2014**, *16*, 2741.
DOI: [10.1007/s11051-014-2741-3](https://doi.org/10.1007/s11051-014-2741-3).
26. Sark, W. V. et al., *ChemPhysChem*, **2002**, *3*, 871 .
DOI: [10.1002/1439-7641\(20021018\)3](https://doi.org/10.1002/1439-7641(20021018)3)
27. Kobliska, R. J. et al , *Phys. Rev. Lett.*, **1972**, *29*, 725.
DOI: [10.1103/PhysRevLett.29.725](https://doi.org/10.1103/PhysRevLett.29.725)
28. Campbell, I. H.; Fauchet, P. M.; *Solid State Commun.*, **1986**, *58*, 739.
DOI: [10.1016/0038-1098\(86\)90513-2](https://doi.org/10.1016/0038-1098(86)90513-2)
29. Mukherjee, S.; Pradhan, A.; Mukherjee, S.; Maitra, T.; Navak, A.; and Bhunia, S., *AIP Conf. Proc.*, **2016**, *1728*, 020111.
DOI: [10.1063/1.4946162](https://doi.org/10.1063/1.4946162)
30. Jiang, J.; Chen, K.; Huang, X.; Li, Z.; Feng, D., *Appl. Phys. Lett.*, **1994**, *65*, 1799.
DOI: [10.1063/1.112848](https://doi.org/10.1063/1.112848)
31. Dana, A.; Agan, S.; Tokay, S.; Aydmh, A.; Finstad, G., *Phys. Status Solidi*, **2007**, *4*, 288.
DOI: [10.1002/pssc.200673233](https://doi.org/10.1002/pssc.200673233)
32. Kasper, J. S.; Richards, S. M., *Acta Crystallogr.*, **1964**, *17*, 752.
DOI: [10.1107/S0365110X64001840](https://doi.org/10.1107/S0365110X64001840)
33. Gorokhov, E.B.; Volodin, V.A.; Marin, D.V. et al., *Semiconductors*, **2005**, *39*, 1168.
DOI: [10.1134/1.2085265](https://doi.org/10.1134/1.2085265)
34. Diao, J.; Gal, K.; and Dunn, M. L., *Nat Mater*, **2003**, *2*, 656.
DOI: [10.1038/nmat977](https://doi.org/10.1038/nmat977)
35. Kim, S. J. et al, *J. Mater. Chem*, **2010**, *20*, 331.
DOI: [10.1039/B915841C](https://doi.org/10.1039/B915841C)
36. Adhikary, H.; McIntyre, P. C.; Sun, S.; Pianetta, P. and Chidsey Christopher E. D., *Appl. Phys. Lett.*, **2005**, *87*, 263109.
DOI: [10.1063/1.2158027](https://doi.org/10.1063/1.2158027)
37. Dukovic, G.; Wang, F.; Song, D.; Sfeir, Matthew Y.; Heinz, Tony F. and Brus, Louis E., *Nano. Lett.*, **2005**, *5*, 2314.
DOI: [10.1021/nl0518122](https://doi.org/10.1021/nl0518122)
38. Steinhoff, A. et al, *Nano Lett*. **2015**, *15*, 6841.
DOI: [10.1021/acs.nanolett.5b02719](https://doi.org/10.1021/acs.nanolett.5b02719)
39. Takagahara, T. and Takeda, K., *Phys. Rev. B.*, **1992**, *46*, 23.
DOI: [10.1103/PhysRevB.46.15578](https://doi.org/10.1103/PhysRevB.46.15578)
40. Koch, S. W.; Kira, M.; Khitrova, G. and Gibbs, H. M., *Nat. Mater.*, **2006**, *5*, 523.
DOI: [10.1038/nmat1658](https://doi.org/10.1038/nmat1658)
41. Zarachias, M. and Fauchet, P. M., *Appl. Phys. Lett.*, **1997**, *71*, 380.
DOI: [10.1063/1.119543](https://doi.org/10.1063/1.119543)
42. Giri, P. K.; Bhattacharya, S.; Kumari, S.; Das, K.; Ray, S. K.; Panigrahi, B. K. and Nair, K. G. M., *J. Appl. Phys.*, **2008**, *103*, 103534.
DOI: [10.1063/1.2930877](https://doi.org/10.1063/1.2930877)
43. Galghar, M. and Osterberg, U., *J. Appl. Phys.*, **1993**, *74*, 2771.
DOI: [10.1063/1.354625](https://doi.org/10.1063/1.354625)



A Monthly Journal

Publish your article in this journal

Advanced Materials Letters is an official international journal of International Association of Advanced Materials (IAAM, www.iaamonline.org) published monthly by VBRI Press AB from Sweden. The journal is intended to provide high-quality peer-review articles in the fascinating field of materials science and technology particularly in the area of structure, synthesis and processing, characterisation, advanced-state properties and applications of materials. All published articles are indexed in various databases and are available download for free. The manuscript management system is completely electronic and has fast and fair peer-review process. The journal includes review article, research article, notes, letter to editor and short communications.

Copyright © 2017 VBRI Press AB, Sweden

www.vbripress.com/aml